

PAPER • OPEN ACCESS

## Heat transfer coefficient of nucleate boiling in low concentration level of single and hybrid Al<sub>2</sub>O<sub>3</sub>-SiO<sub>2</sub> water-based nanofluids

To cite this article: M A H Azzat *et al* 2019 *IOP Conf. Ser.: Mater. Sci. Eng.* **469** 012109

View the [article online](#) for updates and enhancements.



**IOP | ebooks**<sup>TM</sup>

Bringing you innovative digital publishing with leading voices to create your essential collection of books in STEM research.

Start exploring the collection - download the first chapter of every title for free.

# Heat transfer coefficient of nucleate boiling in low concentration level of single and hybrid $\text{Al}_2\text{O}_3$ - $\text{SiO}_2$ water-based nanofluids

M A H Azzat<sup>1</sup>, M Z Sulaiman<sup>1,\*</sup>, K Enoki<sup>2</sup> and T Okawa<sup>2</sup>

<sup>1</sup>Faculty of Mechanical Engineering, Universiti Malaysia Pahang, 26600 Pekan, Pahang, Malaysia

<sup>2</sup>Department of Mechanical and Intelligent Systems, The University of Electro-communications, 1-5-1, Chofugaoka, Chofu-shi, Tokyo 182-8585, Japan

\*Corresponding author: [zuhairi@ump.edu.my](mailto:zuhairi@ump.edu.my)

**Abstract.** Experiments were conducted to identify the Heat Transfer Coefficient (HTC) in saturated pool boiling of single and hybrid water-based nanofluids. In these experiments,  $\text{Al}_2\text{O}_3$  and  $\text{SiO}_2$  nanoparticles were selected and diluted into two separate single nanofluids, and they were mixed in a different ratio from 0:100, 25:75, 50:50, 75:25 and 100:0 percent to achieve a final total concentration of 0.001 vol. %. Successively, the mixtures were used to obtain the HTC values through experimental works. In the present work, it was found that in the lowest concentration (0.00025 vol.%) of  $\text{Al}_2\text{O}_3$  nanofluid, the HTC enhanced considerably but deteriorated for  $\text{SiO}_2$  nanofluid. Separately, as for the hybrid nanofluids, the HTCs were dramatically enhanced at the initial stage but slowly deteriorated once the time variation increased, especially in a higher ratio of  $\text{SiO}_2$  nanofluid. The deposition of the nanoparticles onto the surface heater suggested being the main factor, where in the present case, the significant coexisting effect of the deposited hybrid nanoparticles ( $\text{Al}_2\text{O}_3$  and  $\text{SiO}_2$ ) on the heated surface to the changes of  $\Delta T_w$  due to different nanoparticles properties.

## 1. Introduction

Nucleate boiling involves the high heat transfer rates and coefficients of convection which associated with small values of excess temperature. Therefore, it is desirable to operate many engineering devices such as chiller, heat exchange and many more which in the nucleate boiling regime. Currently, there are two significant heat transfer characteristics in the nucleate pool boiling that attracts most of the researchers which are the Heat Transfer Coefficient (HTC) and Critical Heat Flux (CHF). Most of the studies are focusing on the enhancement of the HTC and CHF which gives the significant benefits to the industries. One of the methods is using nanoparticles.

Various of studies about the effect of nanoparticles on the HTC and CHF were conducted after the discovery by You et al. [1] on the heat transfer enhancement that up until more than 100% for saturated pool boiling using  $\text{Al}_2\text{O}_3$ . Several significant factors were identified to affect the heat transfer in the pool boiling especially related to the surface characteristics such as wettability [2–5], capillarity [6], surface roughness [7–9] and porosity [10–13]. All of these factors significantly altered by the nanofluids deposition proces on the heated surface during nucleate boiling. While the reported results



showed in nucleate pool boiling, the heat transfer demonstrated not only an enhancement but also can be deterioration, and their performance depended on the experimental condition [14–16].

Quan et al. [17] indicated that the pool boiling experiment of SiO<sub>2</sub> with surfactant resulted in the deterioration in HTC but drastically increase for CHF. It is differently finding by Kim et al. [15] where both for CHF and HTC for Al<sub>2</sub>O<sub>3</sub> with distilled water was increased for a particular condition, and both also decrease for a particular condition. Separately, Watanabe et al. [18] proved that the HTC was enhanced, but CHF was deteriorated for nanofluids water based due to the nanoparticles deposited on the heater surface.

Based on the reported study by Sulaiman M. Z. et al. [19], the nanofluid was enhanced for Al<sub>2</sub>O<sub>3</sub> nanofluids but deteriorated in a SiO<sub>2</sub> nanofluid. However, there is no experimental work conducted on the hybrid nanofluids to investigate the effect of nanofluids to the increment or reduction in HTC. An extension to that study, the present work will be emphasised on the performance of hybrid nanofluid (Al<sub>2</sub>O<sub>3</sub> and SiO<sub>2</sub> nanofluids) at low concentrations respective to the heat transfer performance.

In this study, an experimental investigation was performed in nucleate pool boiling of water-based nanofluids. Thus, the paper aims to clarify the influence of concentration for single and hybrid nanofluids on the boiling heat transfer and evaluate the possible mechanism that responsible for the HTC enhancement or deterioration.

## 2. Experimental method

### 2.1 Preparations of nanofluids

In this study, Aeroxide Alu C (Al<sub>2</sub>O<sub>3</sub> (Alumina) particle with a size of 13 nm) and Aerosil 90 (SiO<sub>2</sub> (Silica) particles with a size of 20 nm) were chosen as the enhancement ability shown by previous study [19–21]. These two nanoparticles were in white colours and manufactured by Aerosil Corporation. First, the nanoparticles were diluted in a series of low concentrations dilutions as depicted in Table 1. For hybrid nanofluids, the mixture was by mixing Al<sub>2</sub>O<sub>3</sub> and SiO<sub>2</sub> using the ratio shown in Table 2. Then, the nanoparticles were weighted on a weight scale (Sartorius Practum213-1S) and then mixed with 75 ml of distilled water in a cup. The solution was stirred by hand for several seconds to make sure the nanoparticles adequately dispersed in the distilled water. Then the nanofluid was poured into the 100 ml test tube and then placed in the ultrasonic bath (CPX2800H, Branson). Each dilution was experiencing 1 hour of ultrasonic excitation to get the high stability dispersion of nanoparticles. Later, 75 ml nanofluids were heated up until it achieved its saturation temperature then were injected into the 1425 ml boiled distilled water which located in the test vessel [19].

Table 1: Volume % for single nanofluids

Nanoparticle	Volume %	Type
Al <sub>2</sub> O <sub>3</sub>	0.00025 vol.%	A25
Al <sub>2</sub> O <sub>3</sub>	0.0005 vol.%	A50
Al <sub>2</sub> O <sub>3</sub>	0.001 vol.%	A100
SiO <sub>2</sub>	0.00025 vol.%	S25
SiO <sub>2</sub>	0.0005 vol.%	S50
SiO <sub>2</sub>	0.001 vol.%	S100

Table 2: Ratio of volume % for hybrid nanofluids

Ratio					Types
Nanoparticle	Volume %	Nanoparticle	Volume %	Total volume %	
Al <sub>2</sub> O <sub>3</sub>	0.001	SiO <sub>2</sub>	0	0.001 vol.% : 0 vol.%	A100S0
Al <sub>2</sub> O <sub>3</sub>	0.00075	SiO <sub>2</sub>	0.00025	0.00075 vol.% : 0.00025 vol.%	A75S25
Al <sub>2</sub> O <sub>3</sub>	0.0005	SiO <sub>2</sub>	0.0005	0.0005 vol.% : 0.0005 vol.%	A50S50
Al <sub>2</sub> O <sub>3</sub>	0.00025	SiO <sub>2</sub>	0.00075	0.00025 vol.% : 0.00075 vol.%	A25S75

$\text{Al}_2\text{O}_3$	0	$\text{SiO}_2$	0.001	0 vol.% : 0.001 vol.%	A0S100
-------------------------	---	----------------	-------	-----------------------	--------

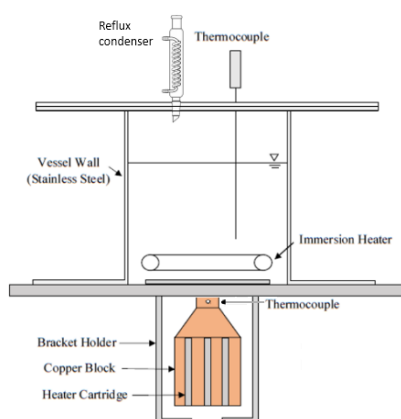
## 2.2 Experimental apparatus

In the present experiment, an experimental setup was fabricated nucleate boiling to investigate the boiling performance in nanofluids. The test sections consisted of a cylindrical vessel, a Perspex cover, a copper block attached with cartridge heaters, several copper block holders, several thermocouples and ceramic fiber insulation blanket. The detail schematic diagram and a photo of the experimental apparatus were shown in Figure 1 (a) and (b).

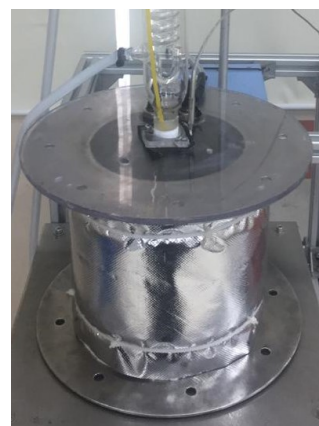
The main body, the vessel, was made from stainless steel with a thickness of 3 mm and the outer diameter of 145 mm of inner cylindrical diameter and the height of the vessel was 185 mm. Outside the cylindrical vessel, the outer surface was covered with thick ceramic fiber insulation blankets. At the bottom of the cylindrical vessel, a heating component was mounted concentrically. A modified one end of the copper block from 40 mm original diameter and shaped it to the cylindrical shape of 20 mm diameter. The copper block surface was used as the heater surface and was in direct contact with the fluids in the main vessel. This copper block attached with a circular stainless-steel plate as a flange with an outer diameter of 100 mm and holes through the middle 20 mm diameter hole. Both components assembled and cured with a reliable and high temperature resistant resin to keep the heater block and stainless-steel flange attached as well as eliminating the clearance gap.

Three type-K thermocouples were positioned along the central axis at this copper end to measure the temperature in the copper block which determines the heat flux,  $q_w$  and wall temperature,  $\Delta T_w$ . The thermocouples were inserted into the drilled holes from top to bottom. While for the other end of the copper block, drilled four holes and inserted cartridge heater (900 W) into all the holes. The copper block was attached to 3 holders to prevent from a slip throughout the experiments. The copper heater and the holder were wrapped a with several layers of ceramic fiber insulation blankets with an anti-burning layer sheet covering outside. The cover was made from Polycarbonate sheet with 6 mm thickness and 250 mm diameter. Using the uncertainty analysis method described by Cooke et al. [22], the measurement uncertainties of  $q_w$  and  $\Delta T_w$  were estimated within less than 84 kW/m<sup>2</sup> and 2.4 K, respectively.

Additional immersion heater with 1 kW was attached to the top cover and located concentrically at the centre of the lower part of the vessel. The immersion heater used to maintain the bulk liquid temperature in the vessel at the saturation condition. A Reflux condenser was equipped on the top cover to prevent the vapour from the test vessel and its cooled with tap water circulation. The pressure inside the vessel was assumed to equal to the atmospheric pressure as the top condenser was open to the atmosphere. Another type-K thermocouple was attached to the cover with its end enter into the vessel. The thermocouple's end was positioned close to the outer diameter of the modified copper surface. A 5 mm diameter hole was drilled onto the top cover, functioned to allow the injection of nanofluid into boiling water in the vessel by using a syringe, then the hole was closed with a rubber plug except during the nanofluid injection.



(a) Schematic diagram



(b) Photo

Figure 1: Experimental apparatus

### 2.3 Experimental procedure

The experiment began with preparation of the heated surface. The heated surface was polished by using metal polishing paste and Kim Wipes, and successively with the surface cleaning by using acetone. Then the vessel cylinder was mounted. Later, the first variable transformer that was attached to the cartridge heater was regulated to supply a  $600 \text{ kW/m}^2$  of heat flux to the copper block. After that, 1425 ml of distilled water were poured into the vessel, and the vessel was closed using Polycarbonate sheet cover attached on the top. Next, the second variable transformer that attached to the immersion heater was regulated to the maximum capacity of 1 kW to boil and degas the distilled water. In order to keep the water level inside the vessel and eliminate the evaporated liquid to escape during the experiment, a Reflux condenser used to condense the water, and it was attached in the middle of the Polycarbonate cover. The degassing process was set to be 20 minutes for each experimental work, and the voltage output from the variable transformer for immersion heater was reduced to the appropriate level enough to keep the water at the saturated condition.

In this experimental stage, the copper block temperature and fluids temperature were measured and monitored by using a temperature module datalogger from National Instrument and DASY LAB software, respectively. The temperatures data were used to calculate the value of wall superheat,  $\Delta T_w$  and the steady state condition was determined by observing the scattering of the  $\Delta T_w$  value in the experimental run was about less than 0.3 degrees C for the approximate duration of 10 minutes. Finally, after a steady state of the copper block was confirmed, the experiment was ready for the next step.

Since the experimental procedures were repeated for each experimental run, the scattering of  $\Delta T_w$  was non-negligible in a separate experimental run since the condition of the heated surface could not be the same. In the experimental setup, the mean  $\Delta T_w$  was found to be in the range of  $14 \pm 2 \text{ }^\circ\text{K}$  and at this state, the nanofluids addition was conducted. This step was necessary because it reduced the influence of the scattering of the initial wall superheat. Separately, the prepared nanofluids in a test tube were heated in another hot boiling water to ensure that the temperature of the nanofluid did not affect the saturated temperature of the distilled water in the vessel. Once the steady state condition was of the copper block was confirmed, the nanofluid was poured into the vessel by using the modified funnel syringe through a small hole located at the top cover of the vessel. After that, the hole was closed with a rubber plug, and the experiment was run for 1 hour, and temperatures were recorded for every second and the time variation of wall superheat,  $\Delta T_w$  was analysed.

## 3. Result and discussion

### 3.1 Effect of concentration variations at relatively low concentration level to the HTC in single nanofluids

Figure 3.1 depicted the time variation of wall superheat  $\Delta T_w$  for two types of single nanofluids ( $\text{Al}_2\text{O}_3/\text{water}$  and  $\text{SiO}_2/\text{water}$ ) in several levels of low concentrations between 0.00025 and 0.001 volume %. They were coded to be A25, A50, A100, S25, S50 and S100 as described in the previous section (see Table 1). Boiling time  $t_b$  was set to be the time duration after the injection of nanofluids into the vessel with a duration of 1 hour present experimental setup. As can be seen, the initial  $\Delta T_w$  of distilled water achieved steady state from the beginning and did not change upon the addition of 75 ml distilled water from the test tube, and it is considered as a reference line. While one could noticeable seen that  $\Delta T_w$  drastically change once the nanofluid was added as shown in Figure 3.1 (a) and (b).

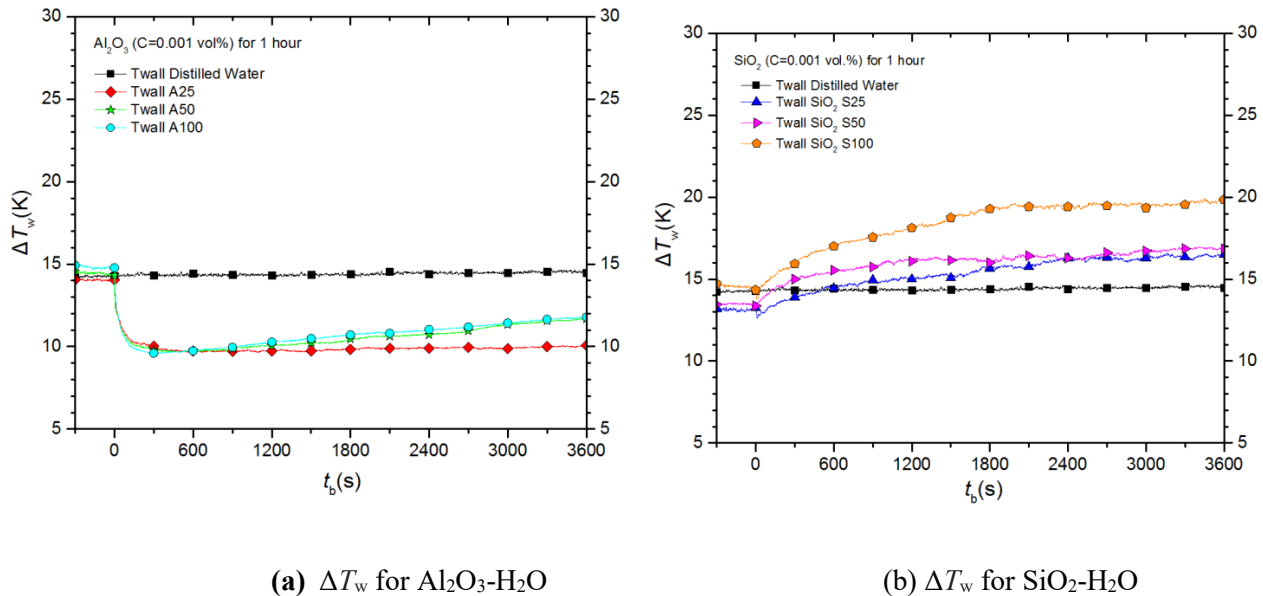
(a)  $\Delta T_w$  for Al<sub>2</sub>O<sub>3</sub>-H<sub>2</sub>O(b)  $\Delta T_w$  for SiO<sub>2</sub>-H<sub>2</sub>OFigure 3.1: Time-variations of wall superheat after adding single nanofluids ( $q_w = 600 \text{ kW/m}^2$ )

Figure 3.1(a) demonstrated the time variation of wall superheat after the injection of Al<sub>2</sub>O<sub>3</sub>/water nanofluid. As can be seen, the  $\Delta T_w$  was instant and sharply reduced after the nanofluid addition for all low level concentration of Al<sub>2</sub>O<sub>3</sub> nanofluid. The results indicate for all those three levels of the low concentrations; each respective  $\Delta T_w$  were kept lower than the distilled water after 1 hour. One could notice that  $\Delta T_w$  for A50 and A100 show similar patterns where after sharp reduction of  $\Delta T_w$  value at the earlier stage a gradually increased trend could be seen after 10 minutes of experiments and end up at the same  $\Delta T_w$  after 1 hour. It could be seen that and they need longer than 1 hour to reach the steady state conditions. While for A25, the  $\Delta T_w$  was kept low throughout 1 hr experiment duration and maintaining a steady state condition. The figure indicates that the smallest level of concentration (A25) could improve heat transfer dramatically. Although both A100 and A50 also showed similar enhancement at the initial stage, the  $\Delta T_w$  was observed keep on increasing in the 1 hour experimental duration.

Figure 3.1 (b) showed the time variation of wall superheat  $\Delta T_w$  for SiO<sub>2</sub>/water nanofluid with three different low concentrations, coded as S25, S50 and S100. In contrast with  $\Delta T_w$  of Al<sub>2</sub>O<sub>3</sub>/water nanofluid, the addition of SiO<sub>2</sub> seems to increase the value of  $\Delta T_w$ . For a maximum concentration of SiO<sub>2</sub>/water in the present experiment (S100), the value for  $\Delta T_w$  was dropped drastically for a few seconds and increased monotonically after that respect to time. After 30 minutes of experiment duration, it achieved the steady state condition where the value of  $\Delta T_w$  was kept maintained in nearly similar range as shown in Figure 3.1 (b). Similarly to the result for the lowest concentration of SiO<sub>2</sub>/water (S25) in present experiment where in the first few seconds, the  $\Delta T_w$  was decreased drastically but increased monotonically to achieve steady state condition. However, compared to the other two higher concentrations, the value of  $\Delta T_w$  was the lowest along the 1 hour of the experiment. For S50 type, it is unnoticeable in Figure 3.1 (b) that the value of  $\Delta T_w$  dropped for the first few second.

After the nanofluids injection, the graph line seems increased monotonically. All graph lines of three different concentration from SiO<sub>2</sub>/water nanofluids shows the same parallel movement of the  $\Delta T_w$  which increased monotonically. However, for S25 and S50 concentrations still did not achieve the steady state condition and keep on increasing slowly. Therefore, further study must be performed to identify the time needed for these two concentrations of SiO<sub>2</sub>/water nanofluid to achieve steady state.

In the present experiments, it was noticeable that after the presence of Al<sub>2</sub>O<sub>3</sub> and SiO<sub>2</sub> in the based liquids, the wall temperature,  $\Delta T_w$  changed depends on the types of nanofluids and its concentrations, supported by the previous studies [23–27]. It can be seen that the value for  $\Delta T_w$  of Al<sub>2</sub>O<sub>3</sub>/water nanofluid decreased as shown in Figure 3.1 (a), same as reported by Hassanpour et al. [28].

Therefore, the HTC was enhanced in that situation. In contrast with  $\text{SiO}_2\text{-H}_2\text{O}$  nanofluids, the HTC was deteriorated because of the pattern of the graph which keeps on increased more than the reference line respect to time. Although the present experiments used a relatively low concentration of nanofluids; it did affect the ability of HTC in the nucleate pool boiling as proven in Figure 3.1.

### 3.2 Composition ratio effects to the HTC of hybrid ( $\text{Al}_2\text{O}_3\text{-SiO}_2$ )/water nanofluid at low concentration (0.001 vol. %)

Base on the unique result of contradicting HTCs in two types of single nanofluids as discussed in section 3.1, experimental work was extended by mixing two types of particles material called hybrid nanofluids. In the present work,  $\text{Al}_2\text{O}_3$  and  $\text{SiO}_2$  were diluted into a series of combination to obtain a single and hybrid water-based nanofluids in order to investigate their HTCs performance in depth. It should be noted that in some cases especially for both single nanofluids, a similar trend also obtained in the previous investigation by Sulaiman M. Z. et al. [19]. The present water-based nanofluids mixing was labelled as A100S0, A75S25, A50S50, A25S75 and A0S100 (see Table 2).

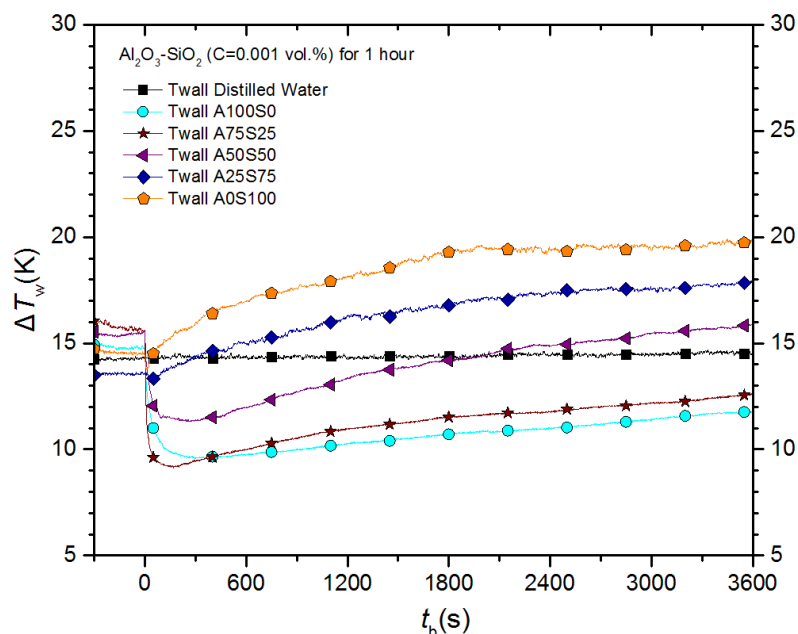


Figure 3.2: Time-variations of wall superheat after adding hybrid nanofluids ( $q_w = 600 \text{ kW/m}^2$ )

Figure 3.2 depicted the result of the wall super heat  $\Delta T_w$  of two single nanofluids and their hybrid at a low-level concentration of 0.001 volume %. For the hybrid nanofluids with type A25S75, the value for  $\Delta T_w$  was dropped first and then slowly increased monotonically respective to time. After 1 hour of experiment duration, the steady state condition was not achieved where the value of  $\Delta T_w$  keep on increasing and the line (marked with a diamond symbol) located on top of the reference line ( $\Delta T_w$  for distilled water) therefore it has a higher value of  $\Delta T_w$  as shown in Figure 3.2. Same goes for the A75S25 type. The figure also demonstrated the  $\Delta T_w$  was slight reduced for all nanoparticles addition in the first few seconds, however at later stage increased asymptotically respective to the time. In the present case, it could be seen that the effect of  $\text{Al}_2\text{O}_3$  showed a considerable reduction in  $\Delta T_w$  especially in the initial stage of nanofluids addition. However, the present of  $\text{SiO}_2$  later diminished the positive effect. For example, one could be seen that in the similar hybrid volume ratio of ( $\text{Al}_2\text{O}_3\text{-SiO}_2$ )/water (A50S50 type), the  $\Delta T_w$  was decreased and gradually shows the increasing value of  $\Delta T_w$ . After 30 minutes, it passed above the  $\Delta T_w$  value of reference line. The trend line for this particular ratio (A50S50 type) falls in the middle of those two single  $\text{Al}_2\text{O}_3$ /water and  $\text{SiO}_2$ /water nanofluids. It is interesting to note that, the  $\Delta T_w$

after 1 hour boiling time were at the consistent magnitude and depended on the ratio of nanofluids mixture. Therefore, it can be concluded that after the injection of hybrid nanofluids, the HTC was enhanced at the beginning, however, the HTC starts to deteriorate slowly respect to time.

Many possible reasons lied in these peculiar trends of the different  $\Delta T_w$  between both types nanofluid ( $\text{Al}_2\text{O}_3$  and  $\text{SiO}_2$  nanofluids). Since the intial addition of nanofluids into the main vessel, the  $\Delta T_w$  decreased drastically due to the nanoparticle deposition process onto the heater surface and possibly promoted activation of new active nucleation sites. Consequently, the heat transfer from heater surface to the liquid was enhanced as discussed by several researchers, i.e. in appendix A in M. Z. Sulaiman et al. [19] and Suriyawong et al. [29]. Similar to the present experiment, the number of active nucleation sites were possibly increased after the addition of the nanofluids even for the lowest concentration of  $\text{Al}_2\text{O}_3$ /water (A25) in the present experimental work. However, in other cases, Suriyawong et al. [29] revealed that 0.0001 vol.% of concentration, the HTC was not affected after the additional of nanofluids because there was no deposition of nanoparticle occur on the heater surface. However, there is an argument about the increase in the number of active nucleation sites by Raveshi et al. [30] where he suggested that the porous nanoparticle layer reduced the nucleate site density and affected the enhancement of HTC multiplying cavities to smaller sites [31].

As for the highest ratio of  $\text{Al}_2\text{O}_3$ /water (A100), the HTC was enhanced considerably with slight deterioration could be seen as boiling time increased. It is most probable to infer that the deposition of  $\text{Al}_2\text{O}_3$  nanoparticle with low thermal conductivity onto the heater surface lowered the HTC value. In addition, the  $\text{SiO}_2$  nanofluid with lower thermal conductivity had demonstrated different characteristics compared to  $\text{Al}_2\text{O}_3$ /water nanofluid where after the injection of nanoparticles, the HTC at the initial stage was slightly increased, but the deposition of  $\text{SiO}_2$  nanoparticle onto the heater surface was increased and resulted in the increasing of thermal resistance [32] and caused the HTC to reduced. For hybrid nanofluids, the active nucleation sites were increased at the initial stage due to the effect of improvement of the surface microstructure, however, the deposition of the  $\text{SiO}_2$  impeding the positive effect from new active nucleation site activation and forming a thicker layer on top of the surface over the time. Consequently, the transient conduction beneath the bubbling bubble was distracted and the HTC was slowly reduced.

#### 4. Conclusions

Experiments were conducted to investigate the heat transfer characteristics for nucleate pool boiling of two single nanofluids ( $\text{Al}_2\text{O}_3$ /water and  $\text{SiO}_2$ /water) and their hybrid at low level concentration of 0.001 vol.%. The heat transfer characteristics in these experiments represented by the time-variation of the wall superheat during nucleate boiling. Main conclusions of this work were summarised as follows.

- a) In most cases in all of the experiments, the wall superheat first decreased drastically and after a few second, it started to react depends on the type of nanofluids (except for the higher composition of  $\text{SiO}_2$ ). For  $\text{Al}_2\text{O}_3$ /water nanofluid, the HTC was enhanced and stable for type A25. However, for types A50 and A100, HTC was enhanced at first and then slowly deteriorates respectively with times. Even though the  $\text{Al}_2\text{O}_3$  nanoparticle deposited on the heater surface will increase the active nucleation site, but due to the high volume of the nanoparticle deposited layer on the heater surface, the HTC observed to slightly decreased over a longer time duration.
- b) For the  $\text{SiO}_2$ /water experiment, the HTC deterioration was observed for in all concentration, but the final value of  $\Delta T_w$  after  $t_b = 1$  hr were depended on the concentrations value, which higher for high concentration and vice versa. It could be noticeable seen in Figure 3.1 (b) that even in type S25, the HTC was reduced. This could be the inferred that the deposited  $\text{SiO}_2$ /water on the heater surface was thickening the nanoparticles layer on the surface and increased the thermal resistance. Consequently, the heat flows were suppressed from moving from the heater surface to the distilled water.

- c) As for the hybrid nanofluids, the HTC were enhanced at the approximately first 30 minutes. After that, the  $\Delta T_w$  slowly increase and pass over the reference line for all the experiments. First, the  $\text{Al}_2\text{O}_3$  nanoparticle will be deposited on the heater surface and will increase the active nucleation sites, and the HTC was enhanced. However, in longer boiling duration, the  $\text{SiO}_2$  nanoparticle with low thermal conductivity deposited on the heater surface and formed a thicker layer that possibly prevents the transient heat conduction from underneath the bubbling bubbles.

### Conflicts of interest

I declare that there are no known conflicts of interest.

### Acknowledgments

Financial support by Universiti Malaysia Pahang ([www.ump.edu.my](http://www.ump.edu.my)) under RDU160385 and Malaysian Ministry of Higher Education under FRGS (FRGS/1/2017/TK07/UMP/03/1)/(RDU170136) are gratefully acknowledged.

### References

- [1] You S M, Kim J H and Kim K H 2003 Effect of nanoparticles on critical heat flux of water in pool boiling heat transfer *Appl. Phys. Lett.* **83** 3374–6
- [2] Bourdon B, Bertrand E, Marco P Di, Marengo M, Rioboo R and Coninck J De 2015 Wettability influence on the onset temperature of pool boiling : Experimental evidence onto ultra-smooth surfaces *Adv. Colloid Interface Sci.* **221** 34–40
- [3] Wang Y, Luo J, Heng Y, Mo D and Lyu S 2018 International Journal of Heat and Mass Transfer Wettability modification to further enhance the pool boiling performance of the micro nano bi-porous copper surface structure *Int. J. Heat Mass Transf.* **119** 333–42
- [4] Doretto L, Longo G A, Mancin S, Righetti G and Weibel J A 2017 Nanoparticle Deposition during Cu-Water Nanofluid Pool Boiling *Journal of Physics: Conference Series* vol 923
- [5] Hu Y, Liu Z and He Y 2018 Effects of  $\text{SiO}_2$  nanoparticles on pool boiling heat transfer characteristics of water based nanofluids in a cylindrical vessel *Powder Technol.* **327** 79–88
- [6] Kim H, Kim E and Hwan M 2014 International Journal of Heat and Mass Transfer Effect of nanoparticle deposit layer properties on pool boiling critical heat flux of water from a thin wire *Int. J. Heat Mass Transf.* **69** 164–72
- [7] Ali H M, Generous M M, Ahmad F and Irfan M 2017 Experimental investigation of nucleate pool boiling heat transfer enhancement of  $\text{TiO}_2$  -water based nanofluids *Appl. Therm. Eng.* **113** 1146–51
- [8] Dadjoo M, Etesami N and Esfahany M N 2017 Influence of orientation and roughness of heater surface on critical heat flux and pool boiling heat transfer coefficient of nanofluid *Appl. Therm. Eng.*
- [9] Rostamian F and Etesami N 2018 Pool boiling characteristics of silica / water nanofluid and variation of heater surface roughness in domain of time *Int. Commun. Heat Mass Transf.* **95** 98–105
- [10] Kim J, Jun S, Laksnarain R and You S M 2016 Effect of surface roughness on pool boiling heat transfer at a heated surface having moderate wettability *Int. J. Heat Mass Transf.* **101** 992–1002

- [11] Kim S J, Bang I C, Buongiorno J and Hu L W 2007 Surface wettability change during pool boiling of nanofluids and its effect on critical heat flux **50** 4105–16
- [12] Park S D, Moon S B and Bang I C 2014 International Journal of Heat and Mass Transfer Effects of thickness of boiling-induced nanoparticle deposition on the saturation of critical heat flux enhancement *Int. J. Heat Mass Transf.* **78** 506–14
- [13] Kiyomura I S, Manetti L L, Cunha A P, Ribatski G and Cardoso E M 2017 International Journal of Heat and Mass Transfer An analysis of the effects of nanoparticles deposition on characteristics of the heating surface and ON pool boiling of water *Int. J. Heat Mass Transf.* **106** 666–74
- [14] Sarafraz M M and Hormozi F 2015 International Journal of Thermal Sciences Pool boiling heat transfer to dilute copper oxide aqueous nano fluids *Int. J. Therm. Sci.* **90** 224–37
- [15] Kim E S, Jung J and Kang Y T 2013 The effect of surface area on pool boiling heat transfer coefficient and CHF of **27** 3177–82
- [16] Li Y, Liu Z and Zheng B 2015 International Journal of Heat and Mass Transfer Experimental study on the saturated pool boiling heat transfer on nano-scale modification surface *Int. J. Heat Mass Transf.* **84** 550–61
- [17] Quan X, Wang D and Cheng P 2017 An experimental investigation on wettability effects of nanoparticles in pool boiling of a nanofluid *Int. J. Heat Mass Transf.* **108** 32–40
- [18] Watanabe Y, Enoki K and Okawa T 2018 International Journal of Heat and Mass Transfer Nanoparticle layer detachment and its influence on the heat transfer characteristics in saturated pool boiling of nanofluids *Int. J. Heat Mass Transf.* **125** 171–8
- [19] Zuhairi Sulaiman M, Matsuo D, Enoki K and Okawa T 2016 Systematic measurements of heat transfer characteristics in saturated pool boiling of water-based nanofluids *Int. J. Heat Mass Transf.* **102** 264–76
- [20] Sharif M Z, Azmi W H, Redhwan A A M, Mamat R and Yusof T M 2017 Performance analysis of SiO<sub>2</sub> / PAG nanolubricant Analyse de la performance du nanolubrifiant SiO<sub>2</sub> / PAG dans un système de conditionnement d'air automobile *Int. J. Refrig.* **75** 204–16
- [21] Sharif M Z, Azmi W H, Redhwan A A M and Mamat R 2016 Investigation of thermal conductivity and viscosity of Al<sub>2</sub>O<sub>3</sub> / PAG nanolubricant for application in automotive air conditioning Étude de la conductivité thermique et de la viscosité de nanolubrifiant Al<sub>2</sub>O<sub>3</sub> / PAG appliqué au système de conditionnement d'air automobile *Int. J. Refrig.* **70** 93–102
- [22] Cooke D and Kandlikar S G 2016 Pool Boiling Heat Transfer and Bubble Dynamics Over Plain and Enhanced Microchannels **133**
- [23] Neto A R, Oliveira J L G and Passos J C 2017 Heat transfer coefficient and critical heat flux during nucleate pool boiling of water in the presence of nanoparticles of alumina, maghemite and CNTs *Appl. Therm. Eng.* **111** 1493–506
- [24] Milanova D, Kumar R, Kuchibhatla S and Seal S 2017 Heat Transfer Behavior of Oxide Nanoparticles in Pool Boiling Experiment 1–9
- [25] Mengüç M P and Kos A 2017 International Journal of Heat and Mass Transfer The effect of nanoparticle type and nanoparticle mass fraction on heat transfer enhancement in pool boiling **109** 157–66
- [26] Minakov A V, Pryazhnikov M I, Guzei D V, Zeer G M and Rudyak V Y 2017 International Journal of Thermal Sciences The experimental study of nano fluids boiling crisis on cylindrical heaters *Int. J. Therm. Sci.* **116** 214–23

- [27] Xu Z G and Zhao C Y 2015 International Journal of Heat and Mass Transfer Experimental study on pool boiling heat transfer in gradient metal foams **85** 824–9
- [28] Hassanpour M, Vaferi B and Esmaeal M 2018 Estimation of pool boiling heat transfer coefficient of alumina water-based nanofluids by various artificial intelligence ( AI ) approaches *Appl. Therm. Eng.* **128** 1208–22
- [29] Suriyawong A and Wongwises S 2010 Nucleate pool boiling heat transfer characteristics of TiO<sub>2</sub> – water nanofluids at very low concentrations *Exp. Therm. Fluid Sci.* **34** 992–9
- [30] Raveshi M R, Keshavarz A, Mojarrad M S and Amiri S 2013 Experimental investigation of pool boiling heat transfer enhancement of alumina-water-ethylene glycol nanofluids *Exp. Therm. Fluid Sci.* **44** 805–14
- [31] Reza M, Keshavarz A, Salemi M and Amiri S 2013 Experimental investigation of pool boiling heat transfer enhancement of alumina – water – ethylene glycol nanofluids *Exp. Therm. Fluid Sci.* **44** 805–14
- [32] Piroo I L, Rohsenow W and Doerffer S S 2004 Nucleate pool-boiling heat transfer. I: Review of parametric effects of boiling surface *Int. J. Heat Mass Transf.* **47** 5033–44